Mon. Not. R. Astron. Soc. **000**, 000,000 (0000) Printed 2 December 2024 (MN LATEX style file v1.4)

Joint Analysis of CMB Temperature and Polarization Power Spectra

D. Munshi[1,2], A.D. Challinor[2], Olivier Doré[3], D.J.Mortlock[1,2] and G.P. Efstathiou[1]
[1] *Institute of Astronomy, Madingley Road, Cambridge - CB3 OHA, United Kingdom*
[2] *Astrophysics Group, Cavendish Laboratory, Madingley Road, Cambridge CB3 OHE, United Kingdom*
[3] *Institut d'Astrophysique de Paris, 98bis boulevard Arago, 75014 Paris, France*

2 December 2024

ABSTRACT
We present a detailed description of analytical methods associated with the joint maximum likelihood estimation of temperature and polarization power spectra from maps produced by Cosmic Microwave Background (CMB) experiments. We investigate the problem both in pixel space and in harmonic domain. The noise properties and issues related to the partial sky coverage are studied. "Electric" and "Magnetic" separation of CMB polarization are analyzed and issues related to pixelisations are investigated. Generalization of maximum-likelihood method using a multi-grid technique is also discussed.

Key words: Cosmology: theory – cosmic microwave background – Methods: analytical – Methods: statistical –Methods: numerical

1 INTRODUCTION

The Map ⋆ (e.g. Jarosik et al. 1998) and Planck † (e.g. Bersanelli et al. 1996) satellites have the potential to yield enormous amount of information about the physical condition in the early universe. If the temperature and polarization measurements are consistent with inflationary models, these measurements will provide an accurate determination of most of the significant cosmological parameters.

These missions will provide low noise maps of CMB temperature and polarization. The Planck High Frequency Instrument (HFI) is the most sensitive instrument currently being built for the measurement of Cosmic Microwave Background (CMB) Anisotropies. The three frequency channels which are polarization sensitive will provide (143Hz, 217Hz and 353 GHz) a detailed map of full sky foreground emission and also that of CMB contribution. While it will allow a clear detection of CMB polarization in small angular scales, it will also provide valuable constrains at high angular scales where a polarized signal from inflationary gravity wave background is expected in many cosmological scenarios.

Polarization of the CMB is produced by electron scattering, as photons decouple from the primordial plasma (Rees 1968; Kosowsky 1996). Gravitational waves produce 'magnetic' (i.e. curl) and electric (i.e. gradient) polarization components at a comparable level by anisotropic red-shift of photon energy. "Magnetic" polarization is not produced by density perturbations (except probably through weak lensing at smaller angular scales), so detection of a magnetic component would provide very strong direct evidence for the presence of a primordial gravitational wave background (Kamionkowski, Kosowsky, & Stebbins 1997; Zaldarriaga & Spergel 1997) which makes it particularly exciting. Detection of primordial polarization will however take into account the fact that such a decomposition of polarization in magnetic and electric parts are not unique in the presence of boundaries. There are various lose-less separation algorithms which were developed recently to tackle these issues. We will focus on maximum likelihood technique to do a "Electric" and "Magnetic" separation.

An observable polarization-curl signal will be detectable only if inflation took place near GUT scale and not at a lower energy scale. This means that even a null result from sensitive polarization experiments would be quite interesting as it would indicate that inflation did not arise from a phase transition at GUT scale or other quantum gravity effects which also place the inflation epoch at a high temperature. In any case following Planck, precise CMB polarization observation will offer the potential to study physical processes at energies as high as 10^{19} Gev observationally (see Kamionkowski & Kosowsky 1999, and Jaffe, Kamionkowski & Wang 1999 and references there in for a detail discussion). High sensitivity

⋆ http://map.gsfc.nasa.gov/m_mm.htm
† http://astro.estec.esa.nl/planck

polarization maps will also be used to study a wide range of other interesting cosmological physics in addition to probing gravitational waves. The polarization maps can be used as a diagonistic to isolate the peculiar-velocity contribution to degree scale anisotropy (Zaldarriaga & Harari 1995). This information then can be used to discriminate between models which give rise to same temperature perturbations. Polarization information can also be used to probe the ionization history of the universe (Zaldarriaga 1997) and primordial magnetic fields (Kosowsky & Loeb 1996; Harari, Hayword & Zaldarriaga 1996) in addition to cosmological parity violation (Lue, Wang & KamionKowski 1999). Keeping all these aspects in mind clearly a joint analysis of temperature and polarization maps will become a necessity for data reduction pipe line of PLANCK mission.

Observations of CMB sky are generally made using various experimental set up e.g. using ground based instruments, high altitude balloons and satellites. The telescope can be a starlight forward dish telescope such as BOOMERanG (e.g. Netterfield et al.) and Planck (e.g. Bersanelli et al. 1990) differencing experiments, such as COBE (e.g. Smoot et al. 1992) and MAP (e.g. Jarosik et al. 1998) and interferometers such as Cambridge Background Imager (CBI, Padin et al. 2001) and the Degree Angular Scale Interferometer (DASI, Halverson et al. 2001). While interferometric surveys generally covers only a small patch of the sky, observations done using satellites will cover almost the full sky. The analysis of data in any CMB experiment will have to go through many non-trivial stages including map-making, component separation and the power spectra estimation. Microwave sky consists of several distinct astrophysical contribution (Haslam et al. 1982; Schlegel, Finkbinder & Davis et al. 1998; Toffolatti et al. 1998; Sunyaev Zeldovich et al. 1970; see Hu, Sugiyama & Silk 1997 or Barreiro 200 et al. for complete review). The spectral behavior of various components contributing to the microwave sky are however quite distinct. Efficient modeling of these components is possible and are used to separate CMB sky from various foregrounds (e.g. Bennett et al. 1992; Tegmark & Efstathiou 1996; Hobson et al. 1998; Bouchet & Gispert et al. 1999; Jones, Hobson & Lesenby 1999 and Baccigalupi et al. 2000; Stolyarov et al. 2001). Such studies have already been done for small patches of the sky and also for whole sky observations. Issues related to the noise in CMB maps are an important one and are directly related to either the map making process or the power spectra estimation. The noise generically consists of two different contribution. A random white noise which is not difficult to model and a potentially troublesome low frequency component known as $1/f$ noise. While differencing experiments in effect remove the $1/f$ noise during observation, other experimental data including Planck data will have to be *destriped* effectively before they can be analyzed. Telescope characteristics also make their imprints in terms of finite point-spread function or beam smoothing. Most experiments have asymmetric beams which must be accounted for. Sometime an average azimuthally symmetric beam is used to make the analysis. The maximum likelihood based power spectra analysis scheme presented here can effectively analyze a correlated noise and other complicated instrument characteristics.

It is a major challenge to reduce the high quality data generated by present and future CMB observations. Computational requirement for a brute force maximum likelihood analysis is quite high (see e.g. Tegmark & Bunn 1994, Borrill 1999). Several approximate schemes has been suggested in recent past both in the context of maximum likelihood analysis (Dore, Knox & Peel 2001) and other estimators (e.g. Tegmark 1996, Szapudi, Prunet & Colombi 2001, Szapudi et al. 2001, Hivon et al. 2002, Wandelt, Hivon & Gorskii 1998, Lewis, Challinor & Turok 2002, Hansen & Gorski 2002, Hansen, Gorski & Hivon 2002) to bring down the cost of computation. Most of these work concentrate on constructing estimators which are unbiased and are close to being optimum. While Tegmark (1996) has analyzed estimators which are minimum variance (see e.g. Tegmark & de Oliveira-Costa 2001 and Bunn et al. 2002), Szapudi, Prunet & Colombi (2001) and Szapudi et al. (2001) concentrate on designing more general estimators which uses sub-optimal pair weight to increase the speed of computations. Other methods based on pseudo-C_ls depend on computing the transfer function to describe the effect of various observational mask on underlying true-C_ls (Hivon et al. 2002). Approximate methods have also been proposed in the context of maximum likelihood analysis too. In particular it has been shown that both high resolution map-making and the power spectrum estimation can be dealt with in a very efficient manner by using the hierarchical decomposition of the map (Dore, Knox & Peel 2001). The idea is to decompose the map into several sub-maps at different resolution and to estimate the parameters from these maps separately and combine them in an optimum way. For low l, coarse maps are used, thereby reducing the number of pixels that needs to be dealt with. For high l several smaller high resolution maps are used to compute the C_ls from them and then combining these estimates in an optimum way to have the resultant estimate. We plan to incorporate such a multi-grid approach in our joint analysis. Correlation function (Szapudi et al. 2001, Szapudi, Prunet & Colombi 2001) based approaches can shown to be a class of more generalized estimators which use a sub-optimal pair weighting scheme. These class of joint estimators are related to the multi-grid joint maximum likelihood estimators. The KL eigen modes represent a very useful basis in which any analysis can be performed in addition to pixel base and the harmonic base. We study these basis function in terms of the generalized eigen values which describe them, for some simple special class with idealized noise and complete sky coverage.

The paper is arranged as follows. In section 2 we discuss the main issues related to the maximum likelihood estimators when it is used to determine the power spectrum associated with the temperature and polarization maps and their cross correlations. In section 3 we outline the results in pixel basis. Section 4 details the numerical implementation. Discussion of our results are contained in section 5. Appendix A and B contains useful results for constant variance uncorrelated noise and all sky coverage which can be very useful for testing and development of the software.

2 MAXIMUM LIKELIHOOD ESTIMATOR

The likelihood function can be written as:

$$\mathcal{L}(C_l^T, C_l^E, C_l^B, C_l^X \mid \mathrm{x}) = \frac{1}{(2\pi)^{\mathrm{N_{pix}}/2}(\mathrm{det}\mathbf{C})^{\mathbf{1/2}}}\exp(-\frac{1}{2}\mathbf{x^T C^{-1} x}). \quad (1)$$

Where $\mathcal{L}$ is the likelihood function, $\mathbf{x}$ is the noisy data vector which composed of either temperature information or the temperature and polarization information in real space or in harmonic space. The covariance between the data vector is described by the covariance matrix C. The goal is to maximize the function $\mathcal{L}$ by varying the parameters C_l^T, C_l^E, C_l^B and C_l^x. The covariance matrix contains the information of both signal or the noise.

Ideally one would like to evaluate the full log-likelihood function over some hypercube in the space of parameters. In this way the global maximum is obtained and also the presence of any local maximum are known immediately. Unfortunately, numerical evaluation of a log likelihood function in the whole parameter space is not practical for the high computational cost associated with it. It is customary therefore to generally to restore to numerical maximization of the log-likelihood function instead. The main disadvantage of course here is that it will converge to the nearest local maxima. One would however hope that the likelihood function is sufficiently structure-less that this is not a reasonable guess for the CMB power spectrum.

Standard minimization(maximization) algorithms use differing amount of information about first and second derivative of the function being minimized (see e.g. Stuart, Ord & Arnold 1994, Press et al. 1999). For example some algorithms such as Powell's direction-set algorithm or the down simplex methods do not use any gradient information and requires only the function evaluation. Other methods which require only the information of the gradient are also valuable if calculation of the first derivative is straight forward. Variable metric method belongs to this category. More popular Newton Raphson techniques which we use for our purpose are based on the calculation of both gradient and curvature information.

If we expand the log-likelihood function in a Taylor series as a function of the parameters and keep terms only up to second order we get:

$$f \equiv -2ln\mathcal{L} = \bar{f} + \sum_{l,P}\frac{\partial f}{\partial C_l^P}(C_l^R - \bar{C}_l^R) + \sum_{(l,l')(R,S)}\frac{\partial^2 f}{\partial C_l^R \partial C_{l'}^S}(C_l^R - \bar{C}_l^R)(C_l^S - \bar{C}_l^S) + \ldots \quad (2)$$

.

The signal part of the covariance matrix S and the noise part of the covariance matrix N will have different characteristics. Depending upon weather we decide to choose to work in pixel basis or in the harmonic domain the covariance matrix will contain information about their correlations. While the noise part of the covariance matrix is diagonal in pixel basis the signal part is not. In harmonic domain the situation is opposite in general and the signal matrix is just the C_ls and is diagonal. In general however N can lack any form of symmetry when correlated noise is present for a general scanning strategy. The specific expressions for various segments of covariance matrix will depend on simplifying assumption one makes to do the analysis.

The Fisher information matrix (Fisher, 1935) for joint temperature-polarization analysis can now be written as the expectation value of the second derivative of the negative log likelihood function:

$$\mathbf{F}_{\mathrm{ll'}}^{\mathrm{RS}} \equiv \left\langle \frac{\partial^2 \mathrm{f}}{\partial \mathrm{C}_{\mathrm{l}}^{\mathrm{R}} \partial \mathrm{C}_{\mathrm{l'}}^{\mathrm{S}}} \right\rangle \quad (3)$$

Where $\langle . \rangle$ denote ensemble averaging. The Fisher matrix can be related to the covariance matrix and its derivative with respect to various types of $C_l's$ by the following equation.

$$\mathbf{F}_{\mathrm{ll'}}^{\mathrm{RS}} = \frac{1}{2}\mathrm{Trace}[\mathbf{C}^{-1}(\mathrm{D}_{\mathrm{l}}^{\mathrm{R}}\mathbf{C})\mathbf{C}^{-1}(\mathrm{D}_{\mathrm{l'}}^{\mathrm{S}}\mathbf{C})] \quad (4)$$

Various sectors of the Fisher matrix will contain information about the different components of our input maps, e.g. $\mathrm{F^{TT}}$ will contain all the information about correlations in C_l s and similarly F_{EE} , F_{BB} or F_{XX} will contain the information about C_l related to E, B or X power spectrum. It can be shown that for constant variance noise and complete sky coverage the estimation equations for various types of polarizations decouples and an independent estimation generates an identical result.

$$\frac{\partial \mathrm{f}}{\partial \mathrm{C}_{\mathrm{l}}^{\mathrm{R}}} = \mathrm{x}^T \mathrm{C}^{-1}\ (\mathrm{D}_{\mathrm{l}}^{\mathrm{R}}\mathrm{C})\ \mathrm{C}^{-1}\mathrm{x} - \mathrm{Trace}[(\mathrm{D}_{\mathrm{l}}^{\mathrm{R}}\mathrm{C})\ \mathrm{C}^{-1}] \quad (5)$$

Once we have computed the Fisher Matrix and the first derivative they can be used to iterate to reach a solution. As fisher Matrix contains all the information about the parameters being determined i.e. their variances and cross correlation they can be used to compute the error bars associated with various parameters.

$$\mathrm{C}_{\mathrm{l}}^{\mathrm{R,(n+1)}} = \mathrm{C}_{\mathrm{l}}^{\mathrm{R,n}} - \frac{1}{2}\sum_{\mathrm{l'S}}(\mathbf{F}^{-1})_{\mathrm{ll'}}^{\mathrm{RS}}\frac{\partial \mathrm{f}}{\partial \mathrm{C}_{\mathrm{l}}^{\mathrm{S,n}}} \quad (6)$$

It can be shown that for constant a variance noise and for full sky coverage the estimation is one step process for arbitrary initial guess for power spectrum. In most general case the changes in the parameter in each step is a quadratic form involving the map hence sometime it is also referred to as a quadratic estimator.

A brute force algorithm can be sped up by exploiting various symmetries in the problem.The Newton Raphson method does not require the full inverse correlation matrix but rather $\mathbf{C}^{-1}\mathbf{x}$, which can be expressed in terms of C_N^{-1} and various $C_S^{1/2}$ factors. Where $C = C_S + C_N$ are the signal and the noise contribution to the total covariance matrix. The idea is to compute z using a simple conjugate gradient techniques which iteratively solves the linear system $\mathbf{Cz} = \mathbf{x}$, by generating improved guess and a new search direction which is orthogonal to the previous direction at each step. In general conjugate gradient is

no faster than the ordinary methods, requiring of order N_{pix} iterations with N_{pix}^2 operations per iteration. However this can be sped up. One can make the matrix well conditioned by finding an appropriate preconditioned which allows the series to converge much faster in only few iterations. Oh Spergel and Hinsaw (1999) used a preconditioner $(I + \mathbf{C}_S^{1/2}\tilde{\mathbf{C}}_N^{-1}\mathbf{C}_S^{1/2})$ where $\tilde{\mathbf{C}}_N^{-1}$ is an approximation to the inverse noise matrix in multi-pole space. It was also taken to be azimuthally symmetric and hence proportional to $\delta_{mm'}$ in multi-pole space which makes it block diagonal and possible to invert quickly. In general a choice of preconditioner will have to depend on specific form of noise matrix and the sky mask being used. No detailed study has so far been made for construction of a preconditioner for polarization analysis or a joint temperature and polarization analysis. However it is expected that such an improvement will be quite interesting for a brute-force joint maximum likelihood code.

Question of hitting upon a local minima was investigated by Bond, Jaffe and Knox (1998). It was found that the likelihood function is sufficiently well behaved which guarantees a quick convergence to global minima even with poor initial guess for the input power spectrum. It can understood intuitively. If various C_ls are not strongly coupled with each other the global maxima search becomes one dimensional maxima search for various c_ls. One would then expect such a result to hold also for the joint estimation unless the C_ls are strongly coupled due to partial sky coverage or complex noise characteristics.

3 ANALYSIS IN PIXEL DOMAIN

The observable polarization field is described in terms of the two Stokes' parameter $Q(\theta,\phi)$ and $U(\theta,\phi)$. These parameters will depend on the local choice of the reference frames and can be decomposed in spherical harmonics $Y_{lm}(\Omega_i)$ and their spinorial counterparts ${}_{\pm 2}Y_{lm}(\Omega_i)$, (Landau & Lifshitz 1975, Varshalovich, Moskalev, Khersonskii 1988) with the harmonic coefficients a_{lm}^R (with $R = T, E, B,$ or X).

$$\langle a_{lm}^T a_{lm}^T\rangle = C_l^T\delta_{ll'}\delta_{mm'};\quad \langle a_{lm}^E a_{lm}^E\rangle = C_l^E\delta_{ll'}\delta_{mm'};\quad \langle a_{lm}^B a_{lm}^B\rangle = C_l^B\delta_{ll'}\delta_{mm'};\quad \langle a_{lm}^T a_{lm}^E\rangle = C_l^X\delta_{ll'}\delta_{mm'} \tag{7}$$

Genreically given inflationary model predicts that a_{lm}^R s are Gaussian distributed with zero mean, $\langle a_{lm}^R\rangle = 0$ and their covariance is determined by the power spectra $\langle a_{lm}^R a_{lm}^S\rangle = C_l^{RS}\delta_{ll'}\delta_{mm'}$. We will assume that the cross correlation of temperature or E modes with B modes vanish identically. Although it is quite easy to remove such an assumption in a more complete analysis, computationally such an extension will be quite formidable. The noise characteristics are best described in pixel domain. In case of uncorrelated noise with constant variance we have $\langle Q^2(\theta,\phi)\rangle = \langle U^2(\theta,\phi)\rangle = \sigma_0^2/2$ and for temperature we have $\langle T^2(\theta,\phi)\rangle = \sigma_0^2$. The noise power spectra can be written as $C_l^{T,N} = 4\pi\sigma_o^2/N_{pix}$ and $C_l^E = C_l^B = 2\pi\sigma_o^2/N_{pix}$.

3.1 Data Vector

As stated above the values of Stokes parameters depend on the choice of axes. The Q field is related to the U field by a rotation of 45^0. The data vector for our maximum likelihood analysis in pixel basis will compose of temperature and these two Stokes parameter Q and U at each pixel.

$$\mathbf{x}(\Omega_i) \equiv \begin{bmatrix} T(\Omega_i) \\ Q(\Omega_i) \\ U(\Omega_i) \end{bmatrix} \tag{8}$$

Decomposition the temperature field and the Stokes' parameters, we can write:

$$T(\Omega_i) = \sum_{lm} a_{lm}^T Y_{lm}(\Omega_i) \equiv \mathbf{Y}(\Omega_i)\mathbf{a}^T \tag{9}$$

$$Q(\Omega_i) = -\sum_{lm}(X_{1lm}(\Omega_i)\ a_{lm}^E + i\ a_{lm}^B\ X_{2lm}(\Omega_i)) \equiv -(\mathbf{X_1}(\Omega_i)\mathbf{a}^E + i\mathbf{X_2}(\Omega_i)\mathbf{a}^B) \tag{10}$$

$$U(\Omega_i) = -\sum_{lm}(X_{1lm}(\Omega_i)\ a_{lm}^B - i\ a_{lm}^E\ X_{2lm}(\Omega_i)) \equiv -(\mathbf{X_1}(\Omega_i)\mathbf{a}^B - i\mathbf{X_2}(\Omega_i)\mathbf{a}^E) \tag{11}$$

Where we have introduced the following notations:

$$X_{1lm}(\Omega_i) \equiv \frac{1}{2}({}_{-2}Y_{lm}(\Omega_i) + {}_2Y_{lm}(\Omega_i))\ ;\quad X_{2lm}(\Omega_i) \equiv \frac{1}{2}({}_{-2}Y_{lm}(\Omega_i) - {}_2Y_{lm}(\Omega_i)) \tag{12}$$

${}_{-2}Y_{lm}$ and ${}_2Y_{lm}$ are the spin harmonics of spin ± 2. a_{lm}^T is the spherical transform of the temperature field and a_{lm}^E and a_{lm}^B are known as the "Electric" and "Magnetic" component of the polarization field.

$$T(\Omega_i) = \sum_{lm} a_{lm}^T Y_{lm}(\Omega_i) \equiv \mathbf{Y}(\Omega_i)\mathbf{a^T} \tag{13}$$

$$Q(\Omega_i) + iU(\Omega_i) = \sum_{lm}(\mathbf{a}_{lm}^E - ia_{lm}^B)\ {}_2Y_{lm}(\Omega_i) \equiv {}_2\mathbf{Y}(\Omega_i)(\mathbf{a}^E - i\mathbf{a}^B) \tag{14}$$

$$Q(\Omega_i) - iU(\Omega_i) = \sum_{lm} (\mathbf{a}^E_{lm} + i\mathbf{a}^B_{lm})\ {}_{-2}Y_{lm}(\Omega_i) \equiv {}_{-2}\mathbf{Y}(\Omega_i)(\mathbf{a}^E + i\mathbf{a}^B) \tag{15}$$

The inverse relations relate the two polarizations Q and U defined over a surface of sphere with corresponding E and B field. The decomposition is not unique for partial sky coverage (see Lewis, Challinor & Turok 2001 for a more complete discussion).

$$\mathbf{a}^T = \int_{4\pi} \mathbf{Y}(\Omega)\ T(\Omega)\ d\Omega \tag{16}$$

$$\mathbf{a}^E - i\mathbf{a}^B = \int_{4\pi} {}_2\mathbf{Y}(\Omega)\ (Q(\Omega) + iU(\Omega))\ d\Omega \tag{17}$$

$$\mathbf{a}^E + i\mathbf{a}^B = \int_{4\pi} {}_{-2}\mathbf{Y}(\Omega)\ (Q(\Omega) - iU(\Omega))\ d\Omega \tag{18}$$

So finally we can write the temperature and polarization field on a sphere as follows.

$$\begin{bmatrix} T(\Omega_i) \\ Q(\Omega_i) \\ U(\Omega_i) \end{bmatrix} = - \begin{bmatrix} 1 & 0 & 0 \\ 0 & \cos 2\tau_{ij} & \sin 2\tau_{ij} \\ 0 & -\sin 2\tau_{ij} & \cos 2\tau_{ij} \end{bmatrix} \sum_{lm} \begin{bmatrix} \mathrm{Y}_{lm}(\Omega_i) & 0 & 0 \\ 0 & \mathrm{X}_{1lm}(\Omega_i) & -i\mathrm{X}_{2lm}(\Omega_i) \\ 0 & -i\mathrm{X}_{2lm}(\Omega_i) & \mathrm{X}_{1lm}(\Omega_i) \end{bmatrix} \begin{bmatrix} a^T_{lm} \\ a^E_{lm} \\ a^B_{lm} \end{bmatrix} \tag{19}$$

The angles τ_{ij} describes the orientation of the local coordinate with respect to which the polarization is being measured. At this stage we can treat them as arbitrary. They will depend on the orientation of two different pixels whose correlations are being measured. Temperature being a scalar field orientation is not relevant but it is important for polarization part of the covariance matrix. The angle τ_{ij} and τ_{ji} are in general not the same for an arbitrary pixel pair i and j.

3.2 Construction of the Covariance Matrix and its Derivative

The joint covariance matrix $\mathbf{C}$ for temperature and polarization field in pixel basis can now be expressed as follows.

$$\begin{aligned} &\mathbf{C}_{ij} \equiv \langle \mathbf{x}(\Omega_i)\mathbf{x}(\Omega_j) \rangle \\ &= \sum_{lm} \begin{bmatrix} Y(\Omega_i) & 0 & 0 \\ 0 & \mathrm{X}_{1lm}(\Omega_i) & -i\mathrm{X}_{2lm}(\Omega_i) \\ 0 & -i\mathrm{X}_{2lm}(\Omega_i) & \mathrm{X}_{1lm}(\Omega_i) \end{bmatrix} \begin{bmatrix} C^T_l & C^X_l & 0 \\ C^X_l & C^E_l & 0 \\ 0 & 0 & C^B_l \end{bmatrix} \begin{bmatrix} \mathrm{Y}(\Omega_\mathrm{j}) & 0 & 0 \\ 0 & \mathrm{X}_{1lm}(\Omega_j) & -i\mathrm{X}_{2lm}(\Omega_j) \\ 0 & -i\mathrm{X}_{2lm}(\Omega_j) & \mathrm{X}_{1lm}(\Omega_j) \end{bmatrix} \end{aligned} \tag{20}$$

For each given pair of observed points i, j the covariance matrix will have TT, QQ and UU terms and their cross terms (see Tegmark & de Oliveira-Costa 2001 for construction of quadratic estimators for polarization analysis). We have decomposed these terms in-terms of the spherical harmonics and spin harmonics and the C_ls describing the correlation among various fields.[‡].

$$\mathbf{C}_{ij} = \begin{bmatrix} \mathbf{C}_{TT} & \mathbf{C}_{TQ} & \mathbf{C}_{TU} \\ \mathbf{C}_{QT} & \mathbf{C}_{QQ} & \mathbf{C}_{QU} \\ \mathbf{C}_{UT} & \mathbf{C}_{UQ} & \mathbf{C}_{UU} \end{bmatrix}_{ij} =$$
$$\begin{bmatrix} \mathbf{Y}^*(\Omega_i)C^T_l\mathbf{Y}(\Omega_j) & \mathbf{Y}^*(\Omega_i)C^X_l\mathbf{X_1}(\Omega_j) & i\mathbf{Y}^*(\Omega_i)C^X_l\mathbf{X_2}(\Omega_j) \\ \mathbf{X}^*_\mathbf{1}(\Omega_i)C_l\mathbf{Y}(\Omega_j) & \mathbf{X}^*_\mathbf{1}(\Omega_i)C^E_l\mathbf{X_1}(\Omega_j) + \mathbf{X}^*_\mathbf{2}(\Omega_i)C^B_l\mathbf{X_2}(\Omega_j) & i\mathbf{X}^*_\mathbf{1}(\Omega_i)C^E_l\mathbf{X_2}(\Omega_j) + i\mathbf{X}^*_\mathbf{2}(\Omega_i)C^B_l\mathbf{X_1}(\Omega_j) \\ -i\mathbf{X}^*_\mathbf{2}(\Omega_i)C^X_l\mathbf{X_1}(\Omega_j) & -i\mathbf{X}^*_\mathbf{2}(\Omega_i)C^E_l\mathbf{X_1}(\Omega_j) - i\mathbf{X}^*_\mathbf{1}(\Omega_i)C^B_l\mathbf{X_2}(\Omega_j) & \mathbf{X}^*_\mathbf{1}(\Omega_i)C^B_l\mathbf{X_1}(\Omega_j) + \mathbf{X}^*_\mathbf{2}(\Omega_i)C^E_l\mathbf{X_2}(\Omega_j) \end{bmatrix} \tag{21}$$

Above expression is valid when the polarization is measured in a coordinate which is parallel transported along the line joining the two points. So these axes are aligned along the line connecting the points and perpendicular to them. However the polarizations are measured in a global coordinate system, e.g. aligned along the latitudes and the longitudinal directions (i.e. along $\hat{\theta}$ and $\hat{\phi}$ direction). This will introduce a rotation of the covariance matrix $R(\tau_{ij})$ and $R(\tau_{ji})$ involving the rotation angles τ_{ij} and τ_{ji} which will not affect the TT part of the covariance matrix but will affect the other sectors TU, TQ, QQ, UU etc. We use HEALPIX subroutines to compute these angles. Thus three angles θ_{ij}, τ_{ij} and τ_{ji} completely specify the separation and orientation any two pixel pair.

‡ Where $\mathbf{Y}$ is a $n \times (2l+1)$ dimensional matrix defined as $Y^i_{lm} = Y_{lm}(\hat{r}_i)$. The index i runs over pixels and the indices l, m charectrises various harmonics. So in this notation the legendre polynomials can be written as $P^l = \mathbf{Y_1}\mathbf{Y^*_1}$ and similar results hold for other harmonics and functions F^{10}, F^{11} and F^{12} that we will introduce later. The terms $\mathrm{C}^\mathrm{T}_\mathrm{l}, \mathrm{C}^\mathrm{E}_\mathrm{l}, \mathrm{C}^\mathrm{X}_\mathrm{l}$ etc. can be thought of diagonal matrices which describe the covariance of all sky harmonics. We have not included beam smoothing and pixel window functions in our expressions but it is straight forward to incorporate them in our result.

$$\mathbf{C}_{ij} = \mathbf{R}(\tau_{ij}) \left[\begin{array}{ccc} \mathbf{C}_{TT} & \mathbf{C}_{TQ} & \mathbf{C}_{TU} \\ \mathbf{C}_{QT} & \mathbf{C}_{QQ} & \mathbf{C}_{QU} \\ \mathbf{C}_{UT} & \mathbf{C}_{UQ} & \mathbf{C}_{UU} \end{array} \right]_{ij} \mathbf{R}(\tau_{ji}) \tag{22}$$

As noted before the rotation angle τ_{ij} and τ_{ji} are not same. As many ingredients go into the construction of the covariance matrix, it is important to have some checks about its accuracy. The eigen values of the covariance matrix or the genralised KL eigen values are very useful for this purpose.

For maximum likelihood analysis the construction of the derivatives of the covariance matrix is necessary. The derivative $\mathbf{D}_l^R\mathbf{C}$ is taken with respect to various power spectra which we want to determine. The derivative with respect to temperature i.e. C_l^Ts is given by:

$$\mathbf{D}_l^T\mathbf{C}_{ij} \equiv \frac{\partial C_{ij}}{\partial C_l^T} = \mathbf{R}(\tau_{ij}) \left[\begin{array}{ccc} \mathbf{Y}^*(\Omega_i)\mathbf{Y}(\Omega_j) & \mathbf{0} & \mathbf{0} \\ \mathbf{0} & \mathbf{0} & \mathbf{0} \\ \mathbf{0} & \mathbf{0} & \mathbf{0} \end{array} \right]_l \mathbf{R}(\tau_{ji}). \tag{23}$$

The derivative matrix depends again both on separation angles of various pixels i.e. θ_{ij} and the relative orientations are determined by τ_{ij} and τ_{ji}. Several block of the derivative matrix vanish which can be effectively used to reduce the cost of computation of the Fisher matrix $\mathbf{F}$.

$$\begin{aligned} \mathbf{D}_l^E\mathbf{C}_{ij} &\equiv \frac{\partial C_{ij}}{\partial C_l^E} = \mathbf{R}(\tau_{ij}) \left[\begin{array}{ccc} \mathbf{0} & \mathbf{0} & \mathbf{0} \\ \mathbf{0} & \mathbf{X_1^*}(\Omega_i)\mathbf{X_1}(\Omega_j) & i\mathbf{X_1^*}(\Omega_i)\mathbf{X_2}(\Omega_j) \\ \mathbf{0} & -i\mathbf{X_2^*}(\Omega_i)\mathbf{X_1}(\Omega_j) & \mathbf{X_2^*}(\Omega_i)\mathbf{X_2}(\Omega_j) \end{array} \right]_l \mathbf{R}(\tau_{ji}) \\ \mathbf{D}_l^B\mathbf{C}_{ij} &\equiv \frac{\partial C_{ij}}{\partial C_l^B} = \mathbf{R}(\tau_{ij}) \left[\begin{array}{ccc} \mathbf{0} & \mathbf{0} & \mathbf{0} \\ \mathbf{0} & \mathbf{X_2^*}(\Omega_i)\mathbf{X_2}(\Omega_j) & i\mathbf{X_2^*}(\Omega_i)\mathbf{X_1}(\Omega_j) \\ \mathbf{0} & -i\mathbf{X_1^*}(\Omega_i)\mathbf{X_2}(\Omega_j) & \mathbf{X_1^*}(\Omega_i)\mathbf{X_1}(\Omega_j) \end{array} \right]_l \mathbf{R}(\tau_{ji}) \end{aligned} \tag{24}$$

Although our expressions here are derived for a mode by mode calculation it can very easily be modified to compute band power estimates. Finally the derivative with respect to C_l^X is a traceless matrix which can be written as:

$$\mathbf{D}_l^X\mathbf{C}_{ij} \equiv \frac{\partial C_{ij}}{\partial C_l^X} = \mathbf{R}(\tau_{ij}) \left[\begin{array}{ccc} \mathbf{0} & \mathbf{Y}^*(\Omega_i)\mathbf{X_1}(\Omega_j) & i\mathbf{Y}^*(\Omega_i)\mathbf{X_2}(\Omega_j) \\ \mathbf{X_1^*}(\Omega_i)\mathbf{Y}(\Omega_j) & \mathbf{0} & \mathbf{0} \\ -i\mathbf{X_2^*}(\Omega_i)\mathbf{Y}(\Omega_j) & \mathbf{0} & \mathbf{0} \end{array} \right]_l \mathbf{R}(\tau_{ji}). \tag{25}$$

The sum over index m of spin harmonics can be expressed interms of the associated Legendre polynomials of various order (Zaldarriaga 1998):

$$(\mathbf{Y}^*(\Omega_i)\mathbf{Y}(\Omega_j))_l = \frac{2l+1}{4\pi} P_l(\cos\theta_{ij}) \ ; \tag{26}$$

$$(\mathbf{X_1^*}(\Omega_i)\mathbf{X_1}(\Omega_j))_l = \frac{2l+1}{4\pi} F_l^{12}(\cos\theta_{ij}) \ ; \quad (\mathbf{X_2^*}(\Omega_i)\mathbf{X_2}(\Omega_j))_l = -\frac{2l+1}{4\pi} F_l^{22}(\cos\theta_{ij}) \ ; \tag{27}$$

$$(\mathbf{X_1^*}(\Omega_i)\mathbf{X_2}(\Omega_j))_l = 0 \ ; \quad (\mathbf{Y}^*(\Omega_i)\mathbf{X_1}(\Omega_j))_l = \frac{2l+1}{4\pi} F_l^{10}(\cos\theta_{ij}) \ ; \quad (\mathbf{Y}^*(\Omega_i)\mathbf{X_2}(\Omega_j))_l = -i\frac{2l+1}{4\pi} F_l^{10}(\cos\theta_{ij}). \tag{28}$$

The angle θ is the angle between two unit vector $\hat{r}(\Omega_i)$ and $\hat{r}(\Omega_j)$, $\cos(\theta) = \hat{r}(\Omega_i)\hat{r}(\Omega_j)$. As these functions describe the correlation functions a study of roots of these functions will also be very useful for correlation function based approaches.

These results are based on vary general principles and no symmetry in observed part of the sky or in noise distributions are assumed to derive these relations.

3.3 Construction of the Fisher Matrix

Once we have constructed the covariance matrix $\mathbf{C}$ and its derivative $\mathbf{DC}$ with respect to various parameters it is possible to compute the Fisher matrix for joint analysis. The Fisher matrix for joint analysis of T,E, B and X (denoted by indices R and S) estimation will be a 4 by 4 block matrix.

$$\mathbf{F} \equiv \ \langle \delta C_l^R \delta C_{l'}^S \rangle^{-1} \ = \ \frac{1}{2}\mathrm{Trace}\Big[\mathrm{C}^{-1}(\mathrm{D}_l^R\mathrm{C})\mathrm{C}^{-1}(\mathrm{D}_{l'}^S\mathrm{C})\Big] \ = \ \left[\begin{array}{cccc} \mathbf{F}_{TT} & \mathbf{F}_{TE} & \mathbf{F}_{TX} & \mathbf{F}_{TB} \\ \mathbf{F}_{ET} & \mathbf{F}_{EE} & \mathbf{F}_{EX} & \mathbf{F}_{EB} \\ \mathbf{F}_{TX} & \mathbf{F}_{TX} & \mathbf{F}_{XX} & \mathbf{F}_{XB} \\ \mathbf{F}_{TB} & \mathbf{F}_{BE} & \mathbf{F}_{BX} & \mathbf{F}_{BB} \end{array} \right]_{ll'} \tag{29}$$

By construction the Fisher matrix will be a symmetric matrix which is also true for various blocks of the Fisher matrix. If we are trying to estimate N parameters in our analysis we will have a $N \times N$ blocks in the Fisher matrix. Covariance of

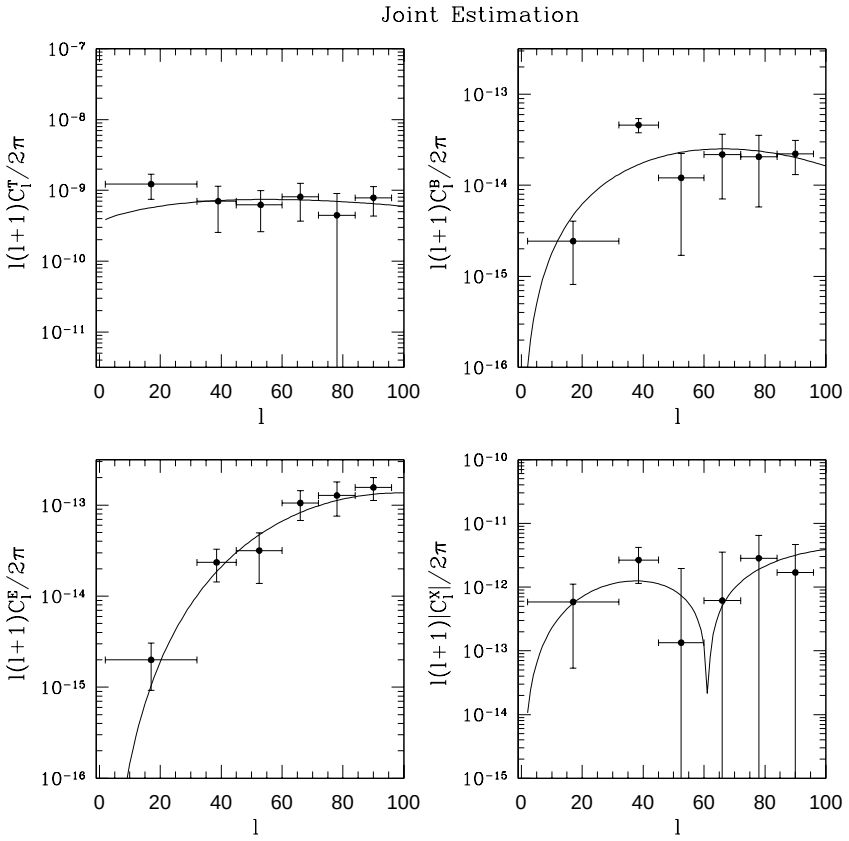

Figure 1. Result of joint maximum likelihood estimation of various power spectra are presented. Solid lines in various panels correspond to target power spectra. Error bars and data points are results from maximum likelihood analysis.

estimated parameters are encoded in these blocks. In general the Fisher matrix will not have any additional symmetry for arbitrary sky coverage and arbitrary noise patterns. However use of azimuthally symmetric noise and sky coverage will induce a block diagonal structure in Fisher matrix. With all sky coverage and constant variance noise various blocks of Fisher matrix will be completely diagonal. As there will be no cross correlation among parameters estimated for same polarization types. For all sky coverage there will be no mixing of modes between B - type polarization and other types of polarizations and hence corresponding blocks (i.e. $\mathbf{F^{BT}}, \mathbf{F^{BE}}$ and $\mathbf{F^{BX}}$) will vanish identically.

Construction of Fisher matrix as described above is most general and can be performed for arbitrary sky coverage and noise properties. However numerical implementation of such a generalized scheme is computationally costly and several approximations have been proposed. These include the minimum variance estimators which uses optimum pair weighing schemes and the approaches based on correlation functions which uses a suboptimal weighing schemes. On the other hand it is possible to extend the above formalism to compute the joint Fisher matrix from various patches independently and combine them in a minimum variance way. It can be shown that it is equivalent to a generalized pair weighing scheme.

4 SIMULATION OF MAPS AND ESTIMATION DETAILS

Simulation of maps were done by using the publicly available software HEALPIX. We used the power spectrum generated by CMBfast to simulate the maps. We show our results for estimations from rectangular maps which are generated from a spherical sky (see Dore et al. 2001 for details). We show results for $N_{side} = 32$ and $N_{side} = 64$. Studies with better resolution can also be performed but with larger band widths. The pixel noise are taken from a Gaussian distribution and we assume zero correlations between pixel pairs. The noise variance is also assumed to be independent of pixel position in the sky. Typically the construction of covariance matrix and its derivative matrix is $O(N_{pix}^2)$ operation for an independent analysis of Temperature maps. For joint covariance it is an order of magnitude higher as the size of the matrix is 9 times bigger. The Fisher matrix computation for polarisation case is $O(10N_{band}^2 N_{pix}^3)$. Where N_{band} is the number of bands and the factor of 10 originates from the fact that there are ten upper triangular blocks which need to be computed. Given this high cost of computation clearly a brute force analysis is unrealistic at the moment for experiments with high resolution and all sky coverage. However as mentioned before the decomposition of Electric and Magnetic polarization will be very useful even for low resolution degraded maps from various experiments aimed at detection of polarisation signals. A detailed analysis of

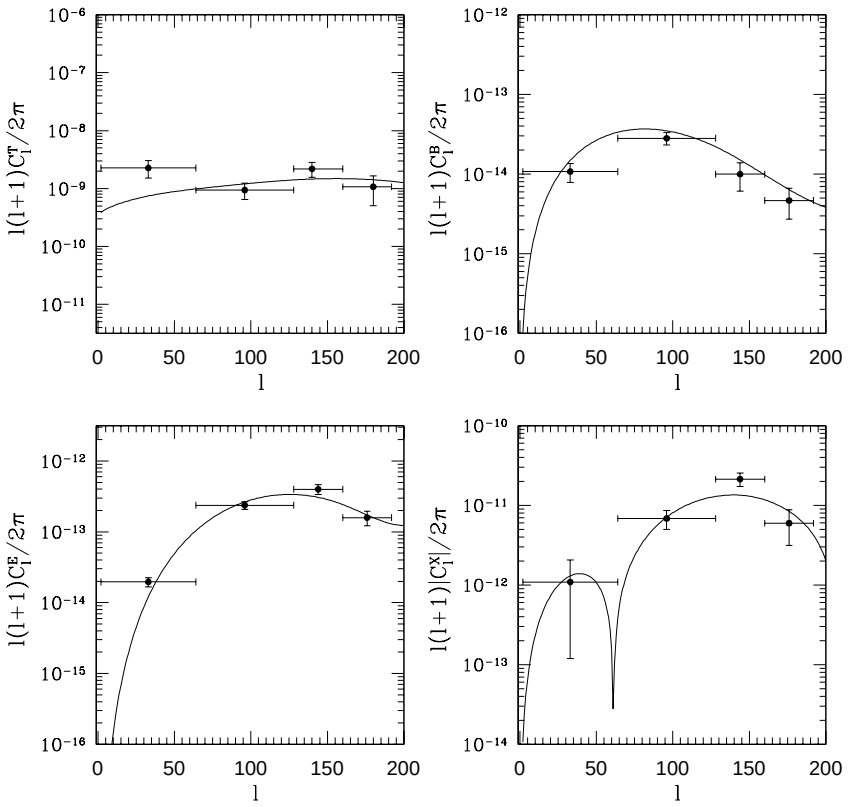

Figure 2. Same as in Figure-1 but for a higher resolution map.

simulated noise for realistic scanning strategy will be presented elsewhere. A brute force maximum likelihood analysis can also be made more efficient by using a hierarchical grid in which case estimators from smaller high resolution maps and larger coarse maps are combined optimally. Pixelisation effects were found to be much more important for analysis of polarization maps compared to temperature maps and must be included during the construction of joint covariance matrix.

5 DISCUSSION

We have implemented a power spectrum estimation method based on the maximum likelihood analysis. Our method is applicable to an independent analysis of temperature and polarization maps or a joint estimation of temperature and polarization maps. We have investigated maximum-likelihood methods which can be used to decompose the contributions from "electric" and "magnetic" type polarization. Maximum likelihood analysis provides a natural way to perform the E and B decomposition in the presence of a boundary or correlated noise. The cross correlations between temperature and polarization maps are also investigated and can be useful for detection of polarization signals.

We have also studied how the presence of various symmetries can simplify the implementation algorithms. In particular we have studied cases where the noise term and the sky coverage has an azimuthal symmetry when the matrix manipulations can be performed in a block by block manner as all matrices become block diagonal. For the case of complete sky coverage and uniform noise, the method is solvable exactly and can work as a test case for software development for both maximum likelihood approach and various approximation schemes.

We have also outlined the connection between various other estimators such as the minimum variance estimators or the estimators based on correlation function analysis in real space and in harmonic domain against the maximum likelihood analysis. We find that a very general class of unbiased estimators for joint analysis can be constructed based on approximation to simplify computations of Fisher matrix.

Our method is suitable for a multi-grid implementation to do a joint analysis of temperature and polarization power spectra (see Dore et al. 2001). A detailed analysis of how such multi-grid approaches are related to heuristic approaches (based on various approximation to pairwise weight function) will be presented elsewhere.

A Fortran 90 implementation of our procedure and its hierarchical decomposition generalization will be made available soon.

ACKNOWLEDGMENT

The COSMOS computing facility was used for the implementation of our parameter estimation code which uses publicly available software LAPAC, HEALPIX and CMBFAST. We would like to thank members of Cambridge Planck Analysis Centre (CPAC) especially Mark Ashdown, Mike Hobson, Vladislav Stolyarov, Floor van Leeuwen and Anthony Lasenby for many useful discussions. DM and DJM were supported by PPARC grant RG28936. ADC acknowledges a PPARC Postdoctoral Research Fellowship. OD acknowledges financial support from "Société de Secours des Amis des Sciences".

REFERENCES

Anderson E. et al. 1992, LAPACK User's Guide. Soc. for Indust. and App. Math. Philadelphia.
Baccigalupi C. et al. 2000, MNRAS, 318, 769
Balbi A., de Gasperis G., Natoli P. & Vittorio N., astro-ph/0203159
Barreriro R. B., 2000, New Astron Rev, 44, 179
Bersanelli M. et al. 1996, COBRAS/SAMBA, The Phase A Study for an ESA M3 Mission. ESA Report D/SCI(96)3
Bond J.R., 1995, PRL, 74, 4396
Bond, J.R., Jaffe, A.H. & Knox, L., 1998, PRD, 57, 2117
Bond, J.R., Jaffe, A.H. & Knox, L., 2000, PRD, 57, 2117
Bond, J.R., Efstathiou, G., & Tegmark, M., 1997, MNRAS, 291L, 33
Borrill, J., PRD, 1999, 59, 027302
Bunn, E.F. & White M., 1997, ApJ, 480, 6
Bunn,E.F., Zaldarriaga,M., Tegmark,M., de Oliveira-Costa, A., 2002, astro-ph/0207338
Challinor, A.D. et al., 2002, MNRAS, 331, 994C
Dore, 0., Knox, L., & Peel, A., 2001, PRD 64, 083001
Eisenstein, D.J., Hu W. & de Oliveire-Costa A., (2000), ApJ, 530, 133
Fisher R.A., J.Roy.Stat.Soc, 1935, 98,39
Gorski, K.M., Wandelt, B.D., Hansen, F.K., Hivon, E., Banday, A.J., astro-ph/9905275
Hansen F.K., Gorski, K.M. & Hivon, E. 2002, astro-ph/0207464
Hansen F.K. & Gorski, K.M., 2002, astro-ph/0207526
Harrai, D.D., Hayward J. & Zaldarriaga M, PRD, 1996, 55, 1841
Haslam C.G.T. Klein U., Salter C.J. Stoffel H., Wilson W.E., Cleary M.N., Cooke D.J., Thomasson P. 1982, A&A, 100, 209
Hobson M.P., Jones A.W., Lasenby A.N., Bouchet F.R., 1998, MNRAS, 301, 1
Hedman M.M., Barkats D., Gundersen, J.O., Staggs S.T. & Winstein B., 2001, ApJL, 548, L111
Hivon, E., Gorski, K.M., Netterfield, C.B., Crill, B.P.,Prunet, S., Hansen, F. 2002, ApJ, 567, 2
Hu W. & White M., New Astron, 323, 2, 323
Hu W. Sugiyama N., Silk J., Nat, 387, 37
Jaffe, A.H., Kamionkowski, M., Wang, L., 2000, PRD, 61, 083501
Lue, A., Wang, L., Kamionkowski, M., PRL, 1999, 83, 1503
Kamionkowski, M., Kosowsky A. & Stebbins A.,1997, PRL, 78, 2058
Kamionkowski, M., Jaffe A.H., 2000, astro-ph/011329
Kamionkowski, M., Kosowsky A. & Stebbins A.,1997, PRD, 55, 1830
Keating, B., Timibie P., Polnarev A., Steinberger, J., 1998, ApJ, 495, 580
Knox, L., PRD, 1995, 48, 3502
Kosowsky A., & Loeb A., 1996, ApJ, 469, 1
Kosowsky, A., 1996, Ann.Phys, 246, 49
Kosowsky, A., astro-ph/9811163
Landau L.D. & Lifshitz E.M., 1975, Quantum Mechanics. Pergamon Press, Oxford.
Lewis A., Challinor A. & Turok N., 2002, PRD, 65, 023505
Mortlock D.J., Challinor A.D., Hobson M.P., 2002, MNRAS, 330, 405
Nutterfield C.B., Devlin M.J., Jarosik N., Page L., Wollack E.J., 1997, ApJ, 474, 47
Nutterfield C.B. et al. 2002 ApJ submitted
Oh, S.P., Spergel, D.N., & Hinsaw G., 1999, ApJ, 510, 551
Press W.H., Teukolsky S.A., Vettering V.T., Flannery, B.P., Numerical Recipes in Fortran 90, (Cambridge University Press, 1999)
Rees, M.J. 1968, ApJL, 153, L1
Seljak, U. & Zaldarriaga M., PRL, 1997, 78, 2054
Smoot G.F. et al., 1992, ApJ, 396, L1
Stolyarov V. Hobson M.P. Ashdown M.A.J., Lasenby A.N. 2002, MNRAS submitted.
Sunayev R.A., & Zeldovich Y.B., 1970, AP& SS, 7,3
Szapudi,I., Prunet S., Pogosyan, D., Szalay A.S., Bond, J.R., 2001, ApJL, 548, L115
Szapudi, I., Prunet S., & Colombi S., 2001, 561L, 11
Tegmark, M. 1996, Apj 464, L35
Tegmark, M., Taylor, A.N. & Heavens A.F.,1997, ApJ, 480, 22
Tegmark, M., Bunn, E.F., 1995, ApJ, 455, 1
Tegmark, M., 1997, PRD, 55, 5895-590
Tegmark & Efstathiou G.P. 1996, MNRAS, 281, 1297
Tegmark, M. & de Oliveira-Costa A. 2001, PRD, 64, 063001
VanLeween F. et al., 2002, MNRAS, 331, 975

Wandelt, B., Hivon E., Gorski, K.M., 1998, astro-ph/9808292
Wandelt, B.D. & Hansen F.K. 2001, astro-ph/0106515
Wandelt, B.D., Hivon, E., & Gorski, K.M., 2000 astro-ph/0106515
Wright, E.L., astro-ph/9612105
Zaldarriaga M. & Seljak U, PRD, 55, 1997, 1830
Zalarriaga, M., Spergel D.N. & Seljak U., 1999, ApJ, 488, 1
Zaldarriaga M., 1998, ApJ, 503, 1
Stuart, A., Ord,J.K., & Arnold, S., Kendel's Advanced Theory of Statistics, vol 2B, (Arnold, London, 1994), 6th Edition
D.M. Brink & Satchler, G.B., Angular Momentum (Clarendon Press, Oxford, 1993), 3rd Ed.
Varshalovich, D.A., Moskalev, A.N. & Khersonskii, V.K., Quantum Theory of Angular Momentum (World Scientific, Singapore, 1988)
Zaldarriaga, M. & Harari D.D., 1995, PRD, 52, 3276
Zaldarriaga, M., 1997, 55 1822

APPENDIX A: UNCORRELATED CONSTANT VARIANCE NOISE AND COMPLETE SKY COVERAGE

Uncorrelated noise with a variance which is same for each pixel, provides an interesting model which can be solved analytically. In this particular case the calculations can be done in a mode by mode manner. It provides a simple test case to check performance of codes meant for more general applicability.

As various l modes are completely independent, we form a $3(2l+1)\times 3(2l+1)$ matrix which represent the covariance between the data vector composed of a^T_{lm}, a^E_{lm} and a^B_{lm} where for each l there are $2l+1$ modes. This reduced covariance matrix will then be a block diagonal matrix, and each of its blocks are just diagonal matrices.

$$\mathrm{C}=\begin{bmatrix}(C_l^T) & (C_l^X) & 0\\ (C_l^X & (C_l^E) & 0\\ 0 & 0 & C_l^B\end{bmatrix};\quad \mathrm{C}^{-1}=\begin{bmatrix}(C_l^{T'})^{-1} & (C_l^{X'})^{-1} & 0\\ (C_l^{X'})^{-1} & (C_l^{E'})^{-1} & 0\\ 0 & 0 & (C_l^{B'})^{-1}\end{bmatrix}. \tag{30}$$

We have considered the matrix for a given m and l but in general there will be a $(2l+1)$ repetition for each m corresponding to a given l. We have assumed that there is no cross talk between B modes and E modes as before which means that the B component of polarization can be handled separately.We have introduces parameters C_l^T, C_l^E, C_l^B and $C_l^{X'}$ for notational simplicity.

$$C_l^{T'}=C_l^T-C_l^X/C_l^E;\quad C_l^{E'}=C_l^E-C_l^X/C_l^T;\quad C_l^{X'}=C_l^X-C_l^EC_l^T/C_l^X;\quad C_l^{B'}=C_l^B \tag{31}$$

The full Fisher matrix can now be computed from these smaller block of covariance matrices corresponding to a particular mode. The Fisher matrix itself will made of various blocks as before. Each diagonal blocks e.g. the TT, EE, BB or XX block will correspond to covariance of estimated C_ls of that particular type and the off-diagonal block will give us the cross correlation between two different types of power spectrum corresponding to a given mode. Diagonal elements of these blocks can be written using parameters defined above as follows:

$$\mathrm{F}^{ll'}_{\mathrm{TT}}=\frac{(2l+1)}{2C_l^{T'^2}}\delta_{ll'};\quad \mathrm{F}^{ll'}_{\mathrm{EE}}=\frac{(2l+1)}{2C_l^{E'^2}}\delta_{ll'};\quad \mathrm{F}^{ll'}_{\mathrm{XX}}=(2l+1)\Big[\frac{1}{C_l^{X'^2}}+\frac{1}{C_l{}^{E'}C_l{}^{T'}}\Big]\delta_{ll'} \tag{32}$$

$$\mathrm{F}^{ll'}_{\mathrm{ET}}=\frac{(2l+1)}{2C_l{}^{X'^2}}\delta_{ll'};\quad \mathrm{F}^{ll'}_{\mathrm{TX}}=\frac{(2l+1)}{C_l{}^{X'}C_l{}^{T'}}\delta_{ll'};\quad \mathrm{F}^{ll'}_{EX}=\frac{(2l+1)}{C_l{}^{X'}C_l{}^{E'}}\delta_{ll'};\quad \mathrm{F}^{ll'}_{\mathrm{BB}}=\frac{(2l+1)}{C_l^{B'^2}}\delta_{ll'}. \tag{33}$$

The inversion of the Fisher matrix can also be done by considering sub matrices corresponding to each mode and it can be directly expressed in terms of the input C_ls of various type.

$$\begin{aligned}&\mathrm{F}^{-1}{}^{ll'}_{\mathrm{TT}}=\frac{2}{(2l+1)}C_l{}^{T^2}\delta_{ll'};\quad \mathrm{F}^{-1}{}^{ll'}_{\mathrm{EE}}=\frac{2}{(2l+1)}C_l{}^{E^2}\delta_{ll'};\quad \mathrm{F}^{-1}{}^{ll'}_{\mathrm{TE}}=\frac{2}{(2l+1)}\frac{(C_l^EC_l^T+C_l^{X^2})}{2}\\ &\mathrm{F}^{-1}{}^{ll'}_{\mathrm{XT}}=\frac{2}{(2l+1)}C_l{}^XC_l{}^T\delta_{ll'};\quad \mathrm{F}^{-1}{}^{ll'}_{\mathrm{XE}}=\frac{2}{(2l+1)}C_l{}^XC_l{}^E\delta_{ll'};\quad \mathrm{F}^{-1}{}^{ll'}_{\mathrm{XX}}=\frac{2}{(2l+1)}C_l{}^XC_l{}^X\delta_{ll'};\\ &\mathrm{F}^{-1}{}^{ll'}_{\mathrm{BB}}=\frac{2}{(2l+1)}C_l^{B^2}\delta_{ll'}.\end{aligned} \tag{34}$$

In general the complete covariance matrix will be have a resolution l_{max} set up by the resolution scale of the map. In which case we will have to do this analysis for each mode and there will be a degeneracy of $2l+1$ for each eigen values.

For computing the eigen values of the derivative matrix, when the derivative is taken with respect to C_l^T,C_l^E and C_l^B the eigen values are just unity. When the derivative is taken with respect to C_l^X the we have eigen values ± 1. Again for each mode we have $2l+1$ eigen values for each of these cases which are all identical. The eigen values of the covariance matrix and its derivative will have to be multiplied by a factor $\frac{4\pi}{N_{pix}}$.

Finally the maximum likelihood estimates can be written as a multi-step root solver in terms of the first order derivative

of the log-likelihood function and its second order derivative which in our case we have approximated with its average. Since power spectra corresponding to T, E and X are correlated, we have to update them simultaneously at each step. Type B polarization however is uncorrelated to other type of power spectra and hence can be dealt with independently for full sky analysis.

$$C_l^{T,(n+1)} = C_l^{T,n} - \frac{1}{2}\Big[(\mathbf{F}^{-1})^{ll'}_{\mathbf{TT}}\frac{\partial f}{\partial C_{l'}^{T,n}} + (\mathbf{F}^{-1})^{ll'}_{\mathrm{TE}}\frac{\partial f}{\partial C_{l'}^{\mathrm{E,n}}} + (\mathbf{F^{-1}})^{\mathbf{ll'}}_{\mathrm{TX}}\frac{\partial \mathbf{f}}{\partial \mathbf{C}_{\mathbf{l'}}^{\mathrm{X,n}}}\Big] \tag{35}$$

$$C_l^{\mathrm{E},(\mathrm{n}+1)} = C_l^{\mathrm{E,n}} - \frac{1}{2}\Big[(\mathrm{F}^{-1})^{\mathrm{ll}}_{\mathrm{ET}}\frac{\partial \mathrm{f}}{\partial \mathrm{C}_{\mathrm{l}}^{\mathrm{T,n}}} + (\mathrm{F}^{-1})^{\mathrm{ll'}}_{\mathrm{EE}}\frac{\partial \mathrm{f}}{\partial \mathrm{C}_{\mathrm{l'}}^{\mathrm{E,n}}} + (\mathrm{F}^{-1})^{\mathrm{ll}}_{\mathrm{EX}}\frac{\partial \mathrm{f}}{\partial \mathrm{C}_{\mathrm{l}}^{\mathrm{X,n}}}\Big] \tag{36}$$

$$C_l^{\mathrm{X},(\mathrm{n}+1)} = C_l^{\mathrm{X,n}} - \frac{1}{2}\Big[(F^{-1})^{\mathrm{ll}}_{\mathrm{XT}}\frac{\partial f}{\partial C_l^{\mathrm{T,n}}} + (F^{-1})^{\mathrm{ll}}_{\mathrm{XE}}\frac{\partial f}{\partial C_l^{\mathrm{E,n}}} + (F^{-1})^{ll}_{\mathrm{XX}}\frac{\partial f}{\partial C_l^{\mathrm{X,n}}}\Big] \tag{37}$$

$$C_l^{B,(n+1)} = C_l^{B,n} - \frac{1}{2}\Big[(\mathbf{F}^{-1})^{ll'}_{\mathbf{BB}}\frac{\partial f}{\partial C_{l'}^{B,n}}\Big] \tag{38}$$

The first order derivative appearing in above expression can now also be written down interms of the input c_l s and the data vector as follows:

$$\frac{\partial f}{\partial C_l^T} = \frac{1}{C_l^{T'^2}}\sum_{m=-l}^{l}|a_{lm}^T|^2 + \frac{1}{C_l^{X'^2}}\sum_{m=-l}^{l}|a_{lm}^E|^2 + \frac{1}{C_l^{T'}\mathrm{C}_{\mathrm{l}}^{\mathrm{X'}}}\sum_{m=-l}^{l}(a_{lm}^T a_{lm}^{*E} + a_{lm}^{*T}a_{lm}^E) - \frac{(2l+1)}{C_l^{T'}} \tag{39}$$

$$\frac{\partial f}{\partial C_l^E} = \frac{1}{C_l^{X'^2}}\sum_{m=-l}^{l}|a_{lm}^T|^2 + \frac{1}{C_l^{E'^2}}\sum_{m=-l}^{l}|a_{lm}^E|^2 + \frac{1}{2C_l^{E'}C_l^{X'}}\sum_{m=-l}^{l}(a_{lm}^T a_{lm}^{*E} + a_{lm}^{*T}\mathrm{a}_{\mathrm{lm}}^{\mathrm{E}}) - \frac{(2\mathrm{l}+1)}{\mathrm{C}_{\mathrm{l}}^{\mathrm{E'}}} \tag{40}$$

$$\frac{\partial f}{\partial C_l^X} = \frac{2}{C_l^{T'}C_l^{X'}}\sum_{m=-l}^{l}|a_{lm}^T|^2 + \frac{2}{C_l^{E'}C_l^{X'}}\sum_{m=-l}^{l}|a_{lm}^E|^2 + \left(\frac{1}{C_l^{T'}C_l^{E'}} + \frac{1}{c_l^{X'^2}}\right)\sum_{m=-l}^{l}(a_{lm}^T a_{lm}^{*E} + a_{lm}^{*T}a_{lm}^E) - \frac{2(2l+1)}{C_l^{X'}} \tag{41}$$

$$\frac{\partial f}{\partial C_l^B} = \frac{1}{C_l^{B'^2}}\sum_{m=-l}^{l}|a_{lm}^B|^2 - \frac{(2l+1)}{C_l^{B'}}. \tag{42}$$

Finally combining all these expressions together and using the expressions for Fisher matrix and its inverse we can show that the joint estimation results can be expressed as follows.

$$\hat{C}_l^T = \frac{1}{2l+1}\sum_{m=-l}^{m=l}\left|a_{lm}^T\right|^2 - C_l^{T,N}; \qquad \hat{C}_l^E = \frac{1}{2l+1}\sum_{m=-l}^{m=l}\left|a_{lm}^E\right|^2 - C_l^{E,N}; \qquad \hat{C}_l^X = \frac{1}{2(2l+1)}\sum_{m=-l}^{m=l}(a_{lm}^{*T}a_{lm}^E + a_{lm}^{*E}a_{lm}^T)$$

$$\hat{C}_l^B = \frac{1}{2l+1}\sum_{m=-l}^{m=l}\left|a_{lm}^B\right|^2 - C_l^{B,N} \tag{43}$$

Which s exactly same as independent estimators. The a_{lm} is the spherical harmonic transform of the noisy map $a_{lm} = a_{lm}^S + a_{lm}^N$ where S denotes the signal part of the contribution and N denotes the noise part of the contribution. Our results can be used for a "quick and dirty" estimation of C_ls with arbitrary cut and noise property (see e.g. Balbi et al. 2002). In which case the noise properties needs to be simulated using a fast map making algorithm and average of noise C_ls can be subtracted directly from spherical harmonic transform of noisy maps whose power spectra are to be computed. The Fisher matrix elements has to be scaled down by changing the number of degrees of freedom from $(2l+1)$ to $(2l+1)f_{sky}$. Where f_{sky} is the fraction of the sky covered in a particular experiment.

APPENDIX B: ANALYSIS OF THE EIGEN VALUES AND ASSOCIATED KARHUNEN-LOÉVE EIGEN VALUE PROBLEM FOR THE JOINT COVARIANCE MATRIX

The construction of polarization co-variance matrix is quite complicated by itself. Various segments of the covariance matrix and its derivative matrix are constructed independently. So it is quite useful to have some checks. Clearly positivity of the covariance is a very crucial test which can always be used as a primary check. Here we list the eigen values of these matrices which are useful diagonistic for any numerical test.

5.1 Eigen values of Covariance Matrix and its Derivative

The eigen value for the matrix are always simpler to compute in the harmonic domain. For all sky calculation with constant variance uncorrelated noise, they can be computed in a mode by mode basis. For a given mode we can write

$$\lambda_i = \frac{1}{2}\Big[C_l^T + C_l^E \pm \sqrt{[(C_l^T - C_l^E)^2 + 4{C_l^X}^2]}\Big], C_l^B \tag{44}$$

As expected the cross correlation between temperature mode and the E-polarization couples various modes however B-modes remain untouched. In case of partial sky coverage however there will be more general mixing of various modes.

The eigen values corresponding to the inverse covariance matrix (which are useful for KL eigen mode analysis or Fisher matrix computation) are given by

$$\lambda_l = \frac{1}{2|D|}\Big[C_l^T + C_l^E \pm \sqrt{[(C_l^T - C_l^E)^2 + 4{C_l^X}^2]}\Big], \frac{C_l^B}{|D|} \tag{45}$$

where $|D|$ is the absolute value of the determinant D of the covariance matrix C corresponding to mode l.

$$D_l = C_l^B(C_l^T C_l^E - {C_l^X}^2) \tag{46}$$

5.2 Analyzing the Karhunen-Loéve Eigen modes

The basic feature of the KL eigen value problem is expansion of the field in a unique set of *statistically* orthogonal spatial functions specific for a given survey geometry and covariance structure of the data and the noise (see e.g. Tegmark, Taylor & Heavens 1997). This analysis can be related to the signal to noise eigen mode analysis and provides a new measure for the power spectra. This method is particularly useful both for CMB observations and galaxy surveys with non-uniform sky coverage which comprise of disjoint regions.

For doing a KL eigen mode analysis one obtains the extrema of $\mathbf{x^t C_{,i}\, x}$ subject to the constraint $\mathbf{x^t C x = 1}$. This is solved by introducing a Lagrangian multiplier λ. The resultant equation is a generalized eigen value problem with v as its eigen vectors.

$$\mathbf{C}_{,i}\,\mathbf{v} = \lambda \mathbf{C v} \tag{47}$$

Where the $\mathbf{C}_{,i}$ is the derivative of the covariance matrix with respect to certain parameter on which the covariance matrix depends. In our case we can take the parameter to be the C_ls themselves for various types of polarization or cross between them. λ is the generalized eigen value for this problem and vector $\mathbf{V}$ lives in the data space and is the KL eigen vector associated with the parameter chosen. The KL eigen mode analysis can also be written as a eigen value problem

$$\mathbf{C}^{-1}\mathbf{C}_{,i}\,\mathbf{v} = \lambda \mathbf{v}. \tag{48}$$

Which is equivalent to a eigen value problem $\mathbf{L^{-1}C_{,i}\,L^{-t}(L^tV)} = \lambda(\mathbf{L^tV})$ of the associated matrix $\mathbf{L^{-1}C_{,i}\,L^{-t}}$ where $\mathbf{C = LL^t}$ is the Cholesky decomposition of the joint covariance matrix $\mathbf{C}$. The KL eigen values do not depend on whether the computations are done in pixel base or in harmonic domain. The $\frac{4\pi}{N_{pix}}$ factors from the inverse covariance matrix and the derivative matrix cancels out.

5.2.1 Eigen modes corresponding to C_l^T, C_l^E or C_l^B

For the case when the derivative is with respect to C_l^T we can write

$$\frac{1}{|D|}\begin{bmatrix} C_l^E & -C_l^X \\ -C_l^X & C_l^T \end{bmatrix}\begin{bmatrix} 1 & 0 \\ 0 & 0 \end{bmatrix} = \lambda \begin{bmatrix} 1 & 0 \\ 0 & 1 \end{bmatrix} \tag{49}$$

and the non-zero eigen value is $\lambda_T = \frac{1}{C_l^{T\prime}}$. Similarly it is easy to check that KL eigen value when the derivative is taken with respect to C_l^E is $\lambda_E = \frac{1}{C_l^{E\prime}}$ and similarly $\lambda_B = \frac{1}{C_l^{B\prime}}$.

5.2.2 Eigen modes corresponding to C_l^X

$$\frac{1}{|D|}\begin{bmatrix} C_l^E & -C_l^X \\ -C_l^X & C_l^T \end{bmatrix}\begin{bmatrix} 0 & 1 \\ 1 & 0 \end{bmatrix} = \lambda \begin{bmatrix} 1 & 0 \\ 0 & 1 \end{bmatrix} \tag{50}$$

So the non-zero eigen values are given by: $\lambda_x^{\pm} = \frac{1}{C_l^{X\prime}} + \frac{1}{\sqrt{C^{T\prime}C^{E\prime}}},\ \ \frac{1}{C_l^{X\prime}} - \frac{1}{\sqrt{C^{T\prime}C^{E\prime}}}$. As before the number of independent eigen modes in KL analysis for a particular type of C_l is $2l+1$ if we assume an uncorrelated noise for each mode.

It can be shown that the new data set is obtained by compressing the original data set $\mathbf{x}$ to a new data set $\mathbf{y = Bx}$ such that y constitute an orthogonal basis set. Where V is the matrix made from the row vectors v and satisfies the matrix equation $C_{,i}\,B^t = CB^t\lambda$ and Λ is the diagonal matrix with entries to the diagonal arranged in a decreasing order. The Fisher matrix F can be associated with the eigen values as:

$$2\tilde{\mathbf{F}}_{ii} = \text{Trace } [\{(\mathbf{BCB^t})(\mathbf{BC_{,i}\,B^t})\}^{\mathbf{2}}] = \text{Trace } \mathbf{\Lambda^2} = \sum_{\mathbf{k=1}}^{\mathbf{n'}} \lambda_{\mathbf{k}}^{\mathbf{2}} \tag{51}$$

The Fisher matrix $\tilde{F}_{ij}$ as expressed as a function of the number of eigen modes used In case the the number of eigen mode n' is same as the dimension of the problem n we get the minimum error bar which also results in a Fisher matrix analysis. In which case $\tilde{F}_{ij}$ becomes identical to F_{ij}.

We have developed the maximum -likelihood analysis in pixel basis and in harmonic domain it is possible to do the similar calculation in the KL basis. This will reduce the cost of computation considerably. However to change basis from pixel basis or from harmonic basis to KL basis in itself is quite costly and will have to take into account. The KL eigen mode analysis however can be very helpful in finding out which combination of modes contain more valuable information for a specific noise model and sky coverage pattern.